A GREEN'S FUNCTION APPROACH TO THE CALCULATION OF DRIFT TUBE CAVITIES*

M. Rich and W. M. Visscher
University of California, Los Alamos Scientific Laboratory
Los Alamos, New Mexico

I. Introduction

We report here on a calculation similar in spirit and method to that of Gluckstern[1] with some simplification and some generalization. Briefly, our method is to first use the symmetries of the drift tube calculation problem to reduce Maxwell's equations to a single one, which we solve by use of a cylindrical Green's function.[2] The Green's function gives directly and exactly the fields inside a cylindrical conductor for a prescribed dipole disc (or tube) source with sinusoidal time dependence of arbitrary frequency. By integrating this Green's function over a source distribution, we can in principle (and, with enough patience, in practice) obtain an exact solution for the fields due to an arbitrary internal current distribution. We have chosen a particular form for the internal current distribution, with which we hope to be able to mock up a variety of drift tube shapes.

Given a current distribution, the fields can be obtained exactly. If the fields have a mode on the transverse plane which bisects the current distribution, then one can start at that point to construct a surface which is everywhere normal to the electric vector. If this surface is found to stay outside of the current distribution, then the fields would be unchanged if the surface were made of a perfect conductor. If the conductor has a reasonable shape, we have designed a drift tube and can easily obtain the shunt impedance and transit time factor by numerical integration.

II. Equations

We define, in cylindrical coordinates

$$r\, B_\theta\,(r, z, t) = e^{i\omega t}\, F\,(r, z)\,. \tag{1}$$

Then for a current

$$\vec{j}\,(r, z, t) = e^{i\omega t}\,\vec{j}\,(r, z)\,, \tag{2}$$

Maxwell's equations reduce to

$$r\,\frac{\partial}{\partial r}\,\frac{1}{r}\,\frac{\partial F}{\partial r} + \frac{\partial^2 F}{\partial z^2} + \frac{\omega^2}{c^2}\,F = \mu_o\, r\left(\frac{\partial j_z}{\partial r} - \frac{\partial j_r}{\partial z}\right) \tag{3}$$

*Work performed under the auspices of the U. S. Atomic Energy Commission.

in MKS units. The Green's function for Eq. (3) satisfies

$$(\mathcal{L} + \lambda^2)\, G(r, z; r', z') = r\, \delta(r - r')\, \delta(z - z') \tag{4}$$

with

$$\mathcal{L} = r \frac{\partial}{\partial r} \frac{1}{r} \frac{\partial}{\partial r} + \frac{\partial^2}{\partial z^2} \quad .$$
$$\lambda^2 = \omega^2/c^2 \, . \tag{5}$$

Upon defining χ_k as a complete set of eigenfunctions of

$$\mathcal{L}\, \chi_k = -k^2 \chi_k \, , \tag{6}$$

G can be formally written down as

$$G(r, z; r', z') = \sum_k \frac{\chi_k(r, z)\ \chi_k^\dagger(r', z')}{\lambda^2 - k^2} \, , \tag{7}$$

which is verifiable by inspection of Eqs. (4) and (6) if the normalization of χ_k is such that

$$\int_0^R \frac{dr}{r} \int_0^L dz\ \chi_{k'}^\dagger(r, z)\ \chi_k(r, z) = \delta_{kk'} \, , \tag{8}$$

where R and L are the cavity radius and half length respectively (see Fig. 1). A complete set of χ_k's satisfying Eqs. (6) and (8) and the boundary conditions imposed by the physics of the problem, namely

$$\chi\Big|_{r=0} = 0$$
$$\frac{\partial \chi}{\partial r}\Big|_{r=R} = 0 \tag{9}$$
$$\frac{\partial \chi}{\partial z}\Big|_{z=0,\, L} = 0$$

is the two-parameter set

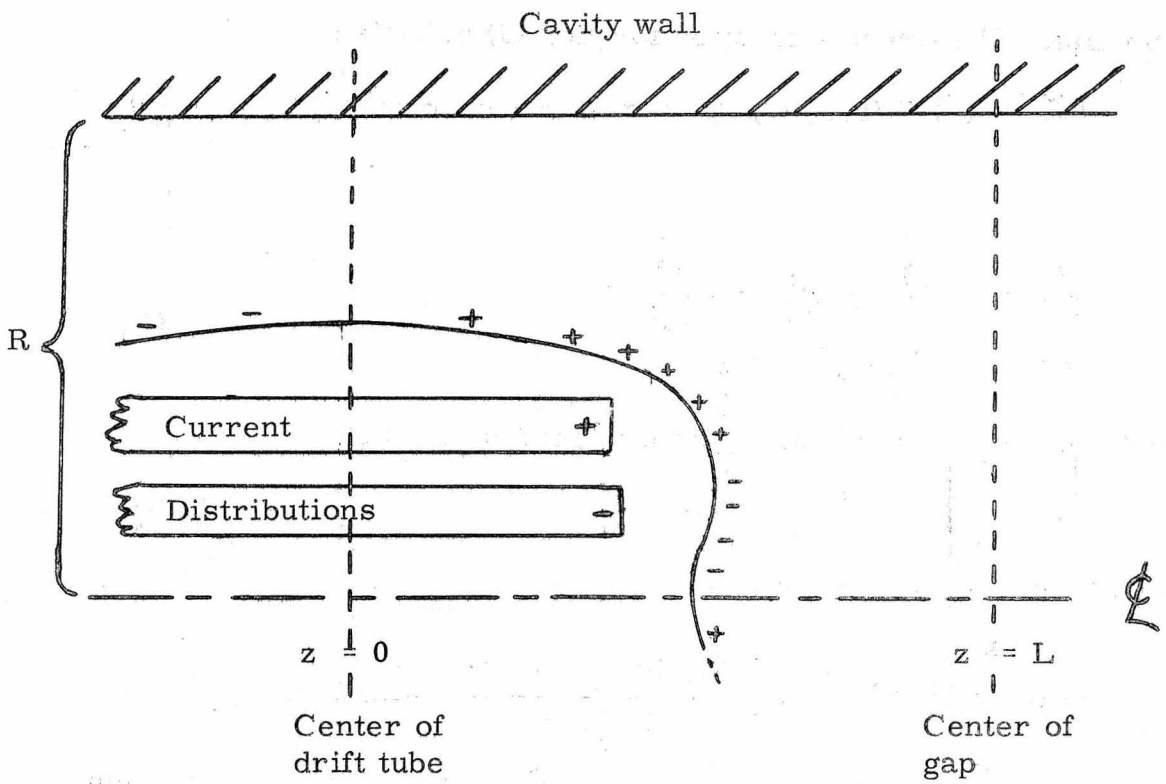

Fig. 1 Unit cell quadrant

$$\chi_{m,n} = \sqrt{\frac{2-\delta_{m,0}}{L}} \cos\frac{m\pi z}{L} \frac{\sqrt{2}}{\rho_n |J_1(\rho_n)|} \rho_n \frac{r}{R} J_1\left(\rho_n \frac{r}{R}\right), \quad (10)$$

where m runs over all the non-negative integers and ρ_n is the n^{th} root of J_0.

Equation (7) is therefore a double sum, over n and m. Either, but not both, of them can be summed in closed form. One of the sums must be left for the computer to do numerically. The choice is made on the basis of speed of convergence; the more slowly converging sum always being done first, analytically. The relevant results are

$$\sum_n \frac{2rr'}{R^2 J_1^2(\rho_n)} \frac{J_1(\rho_n r/R) J_1(\rho_n r'/R)}{\kappa^2 - (\rho_n/R)^2} = \frac{\pi rr'}{2} J_1(\kappa r_<) \left[N_1(\kappa r_>) - J_1(\kappa r_>) \frac{N_0(\kappa R)}{J_0(\kappa R)}\right], \quad (11)$$

or, if $\kappa^2 = -\kappa'^2$ is negative,

$$\sum_n = -rr' I_1(\kappa' r_<)\left[I_1(\kappa' r_>)\frac{K_0(\kappa' R)}{I_0(\kappa' R)} + K_1(\kappa' r_>)\right], \quad (12)$$

where $r_>$ is the greater of r and r' and $r_<$ the lesser of the two. If one wishes to do the sum over m analytically, it is

$$\sum_{m=0}^{\infty} \frac{2-\delta_{m,0}}{L} \frac{\cos\frac{m\pi z}{L}\cos\frac{m\pi z'}{L}}{\beta^2 + \left(\frac{m\pi}{2}\right)^2} = \frac{\cosh\beta(z_> - L)\cosh\beta z_<}{\beta \sinh\beta L}. \quad (13)$$

The solution $F(r,z)$ of Eq. (3) is found from the Green's function according to

$$F(r,z) = \mu_0 \int_0^R dr' \int_0^L dz' \, G(r,z;r',z') \left(\frac{\partial j_z(r'z')}{\partial r'} - \frac{\partial j_r(r',z')}{\partial z'}\right). \quad (14)$$

Here we must specify the form of $\vec{j}$. We stipulate that only j_z differs from zero, and that it has the form

$$j_z(r;z') = \frac{1}{\mu_0}\sum_\mu j_\mu \cos k_\mu z' \, \theta(r' - a_\mu)\,\theta(b_\mu - r')\,\theta(y_\mu - z') \quad (15)$$

where θ is the unit step function $\theta(x) = \frac{1}{2}\left(1 + \frac{x}{|x|}\right)$. Since the derivative of θ is a δ function, the integral over r' in Eq. (14) can be performed by inspection, and the integral over z' is elementary. The task remaining is then to perform either the n or m sum and the μ sum (which we have never yet taken to have more than two terms).

III. Calculations

A Fortran code for the IBM 7094 has been written to calculate drift tube shapes using Eq. (14) for F. The input consists of the parameters of Eq. (15) describing the current distribution, the frequency, the cavity radius, the proton energy (length of the cavity), the surface resistivity of the structural material, and a number to provide a convergence criterion for the Bessel function sums. Since the metallic boundary condition for Maxwell's equations specifies that the normal derivative of F vanish at the surface

$$\frac{\partial F}{\partial n} = 0, \tag{16}$$

and since at z = 0 the surface of the drift tube is parallel to the axis, F must satisfy

$$\frac{\partial F}{\partial r} = 0 \tag{17}$$

at the point r_d where the metal cuts the median plane. The code searches r at z = 0 for a point satisfying Eq. (17); if one is found, it then integrates Eq. (16) to find the surface along which one can put a metallic drift tube without altering the fields. The method used to integrate Eq. (16) is the same as that used by Gluckstern; briefly, it approximates the curve of the surface by a series of circular arcs of constant chord. By reducing the chord length one can increase the accuracy indefinitely; we find 1/2 cm to be usually adequate.

The transit time factor is formed by a Simpson's rule integration of the E field along the axis

$$T = - \frac{\int_0^L \left(\frac{1}{r}\frac{\partial F}{\partial r}\right)_{0,z} \cos\frac{\pi z}{L}\, dz}{\int_0^L \left(\frac{1}{r}\frac{\partial F}{\partial r}\right)_{0,z} dz} . \tag{18}$$

The shunt impedance is found by a Simpson's rule integration of B^2 over the metal surfaces of the drift tube and the outer cylinder:

$$ZT^2 = \frac{(\text{numerator of Eq. (18)})^2}{L\,\omega^2\,\epsilon^2\,\pi\,R_s \int \frac{F^2}{r}\, d\ell} , \tag{19}$$

where $R_s = 3.6 \times 10^{-3}$ ohms for copper at 200 Mc, $\epsilon^{-1} = 36\pi \times 10^9$, and the integral is a line integral over all the metal surfaces in a quarter cell as shown in Fig. 1.

Other output available from this code includes the maximum electric field on the drift tube, the electric fields everywhere in the cavity, and the fraction of the total power dissipation which occurs on the drift tube.

IV. Results

The form of Eq. (15) allows the construction of distributed charge distributions for excitation of a cavity. Except for comparisons with some cases of Gluckstern,[1] the problems which have been run with the present code were done with two charge distributions of opposite sign running parallel to the cavity axis, the lower one usually carrying less charge than the upper. This choice was made with the hope that it would more nearly approximate the charge configuration which must be produced in the metallic surface of a real drift tube, as illustrated by the + and - signs in Fig. 1, in order to result in an interior shielded region. In this we have only been partially successful. Axial indentations in the drift tubes can be accomplished with such dipole charge distributions and the axial fields interior to the drift tubes can be made approximately zero, but the electric fields near the end of the charge distribution and close to the axis vary rapidly in such a way that formation of a true hole seems impossible. Presumably a more complicated charge distribution would produce a drift tube with an axial hole.

No exhaustive study of drift tube shapes has been made with the present code. Some problems have been run at 10, 50, 100, and 150 MeV in an effort to obtain relatively cylindrical drift tubes with reasonable values of $Z\,T^2$, G/L, and radius. Because of the large number of parameters involved with these distributed "dipole" charge distributions and the restriction to reasonable shapes, optimization of the drift tubes becomes very difficult.

Running times with 0.5 centimeter integration stop and a maximum of sixty sum terms are about three minutes per problem. These use a single sinusoidal form for the Z-dependence of each of two distributions. The phase of the cosine function at the end of the distribution was kept the same for both in each case. For similar drift tube sizes and shapes in the neighborhood of what appeared to be optimum, ZT^2 values were not overly sensitive to changes in the parameters of the charge configurations, as would be expected. Relative to an arbitrary configuration in this neighborhood, increasing the cavity radius decreases the drift tube radius, generally with a resultant increase in ZT^2. An increase of the length of the charge distribution would decrease the drift tube radius while slightly increasing its length. As the phase of the sinusoidal charge distributions were made to approach 90°, distributing the charge more uniformly, the drift tube radius would in general increase, reducing ZT^2. Finally, making the magnitude of the charge on the lower distribution approach that of the upper tended to result in a reduction of the drift tube radius and the formation of an indentation at its front, the beginnings of a hole.

Figures 2, 3, 4, and 5 show some typical results for drift tube shapes and axial electric fields within the gap for energies of 10, 50, 100, and 150 MeV, respectively. Pertinent data with respect to cavity radius, g/L, T, ZT^2, etc., are contained in the figures. These results are consistent with those of Gluckstern[1] and with MURA MESSYMESH calculations,[3] although there seems to be a tendency to obtain lower ZT^2 values than do the latter.

In conclusion, we would like to emphasize that the material presented here is very preliminary. It is hoped that as more detailed parameter studies are made and more "realistic" charge distributions used, a closer approach to drift tube optimization will be achieved.

YOUNG: I have two questions. The first is: How much effort have you put into making a drift tube hole and are you going to devote more attention to this? The second is: Have you checked your program against the results of other programs?

VISSCHER: To the first question: We have made an effort to achieve a drift tube hole. I don't think that it is practical for us because we have so many parameters to change to optimize the drift tube shape. By adding one or more current distributions close to the point where the drift tube contour intersects the axis when these currents are not present, we can get a deep depression in the nose of the drift tube, but not a real hole.

As far as our agreement with other calculations that have been done, we have tried to reproduce some of Gluckstern's single-charge drift tube shapes. We were able to do that all right with the agreement in shunt impedance to within a couple of percent. The difference may be due to the fact that we didn't quite duplicate his shape. We can't really duplicate the shapes calculated by the MURA MESSYMESH program but our results are in general agreement considering this fact.

REFERENCES

1. R. L. Gluckstern, Proceedings of the International Conference on Accelerators, Brookhaven National Laboratory, 1961.

2. P. M. Morse and H. Feshbach, Methods of Theoretical Physics, McGraw-Hill Publishing Company, 1953.

3. See, for example, MURA reports 622 and 642.

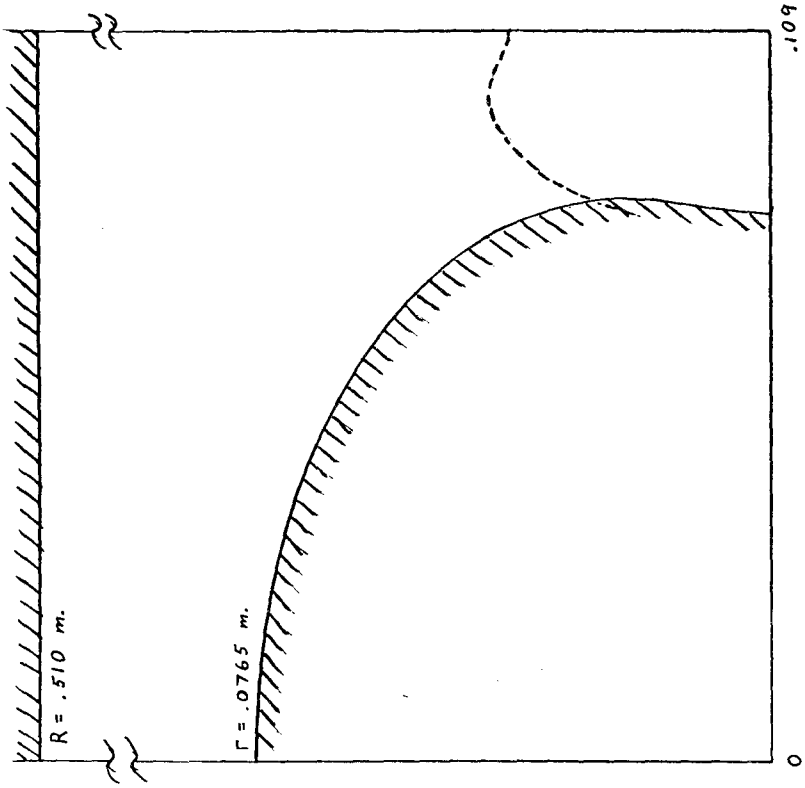

Fig. 2: Example of a 10 Mev drift tube shape and axial E field. E_{max} is the maximum field on the drift tube in units of the field at the center of the gap; f is the fraction of the total RF power dissipated on the drift tube.

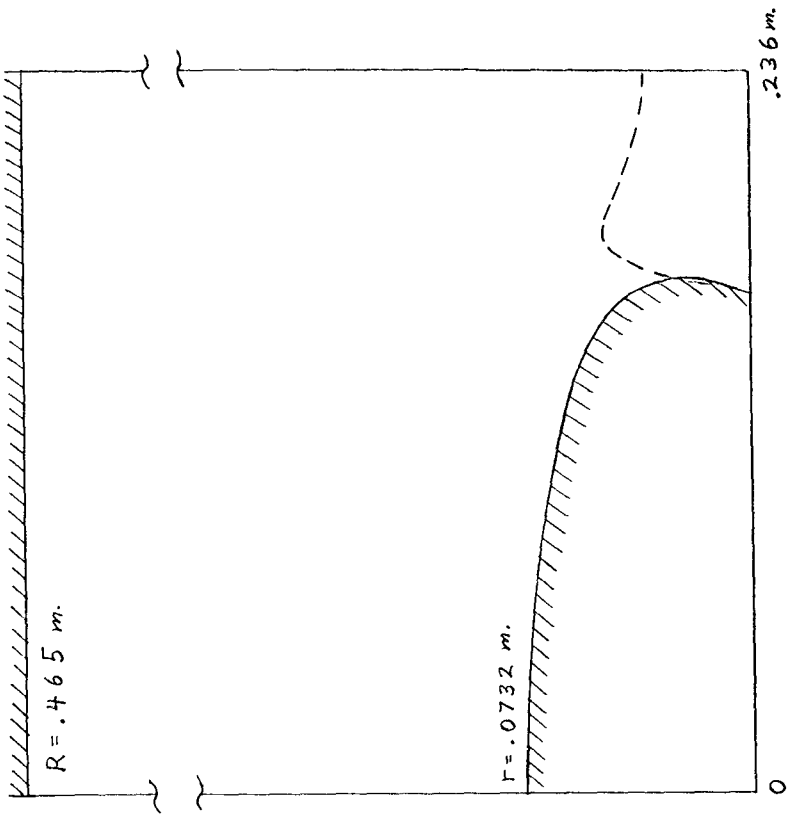

Fig. 3: Example of a 50 Mev drift tube shape and axial E field.

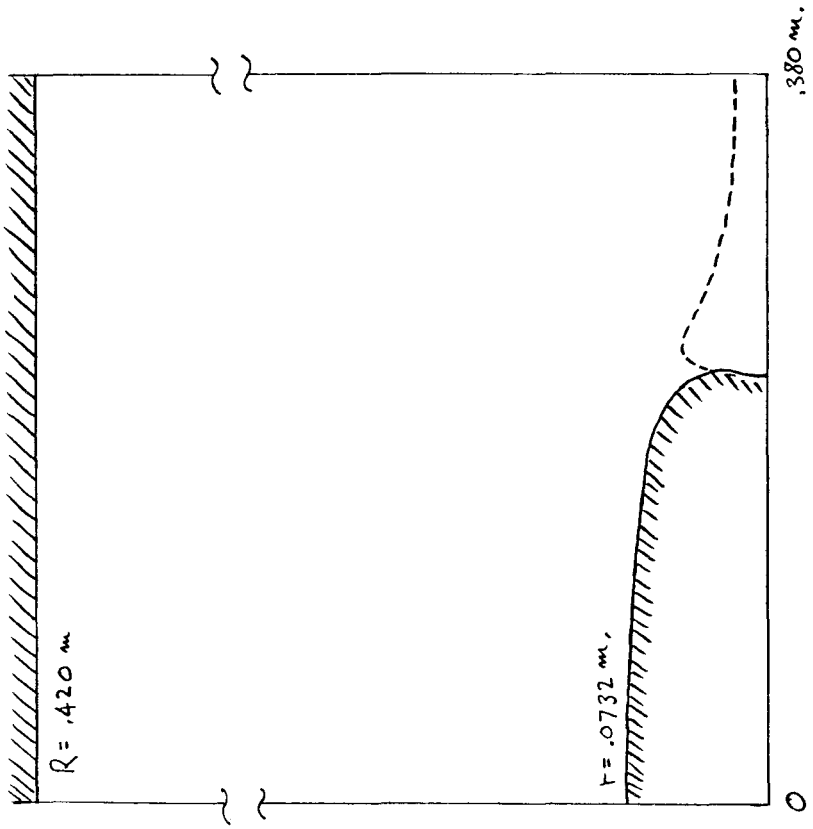

Fig. 5: Example of a 150 Mev drift tube shape and axial E field.

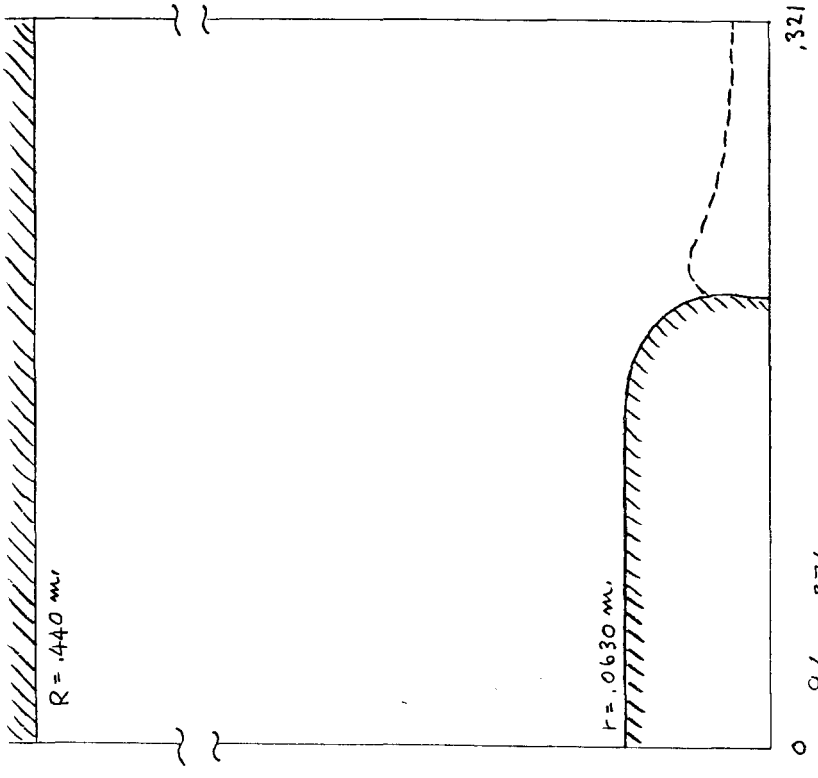

Fig. 4: Example of a 100 Mev drift tube shape and axial E field.